Electronic Supplementary Material (ESI) for Energy & Environmental Science.
This journal is © The Royal Society of Chemistry 2017

Supporting Information

Active Sites Engineering Leads to Exceptional ORR and OER Bifunctionality in P,N Co-Doped Graphene Frameworks

Guo-Liang Chai,*†[ab] Kaipei Qiu,†[ac] Mo Qiao,[d] Maria-Magdalena Titirici,[de] Congxiao Shang,[f] and Zhengxiao Guo*[a]

[a] Department of Chemistry, University College London, London WC1H 0AJ, United Kingdom.

[b] State Key Laboratory of Structural Chemistry, Fujian Institute of Research on the Structure of Matter, Chinese Academy of Sciences, Fuzhou, 350002 Fujian, People's Republic of China.

[c] Renewable Energy Group, College of Engineering, Mathematics and Physical Sciences, University of Exeter, Penryn Campus, TR10 9FE, United Kingdom.

[d] School of Engineering and Materials Science, Queen Mary University of London, Mile End Road, E1 4NS London, United Kingdom.

[e] Materials Research Institute, Queen Mary University of London, Mile End Road, E1 4NS London, United Kingdom.

[f] School of Environmental Sciences, University of East Anglia, Norwich NR4 7TJ, United Kingdom.

1. Formation energy

For P,N doped carbon catalysts, the formation energies are calculated using N_2 gas and P_4 molecules as references for nitrogen and phosphorus, respectively. The formation energies are given by:

$$\Delta E_f(i\mathrm{P}j\mathrm{N}) = E(i\mathrm{P}j\mathrm{N}) - E_0 + (i+j)*E(\mathrm{C}) - (i/4)*E(\mathrm{P}_4) - (j/2)*E(\mathrm{N}_2) \qquad (S1)$$

where i and j are the numbers of the doped P and N atoms, respectively; $\Delta E_f(i\mathrm{P}j\mathrm{N})$ is the formation energy; $E(i\text{P}j\text{N})$ is the total energy of P, N doped structures; E_0 is the total energy of un-doped structures; $E(\text{C})$ is the total energy per atom of perfect graphene; $E(\text{N}_2)$ is the total energy of an N_2 molecule; $E(\text{P}_4)$ is the total energy of P_4 molecule. The formation energies for different structures are shown in **Fig. 2** in the main text.

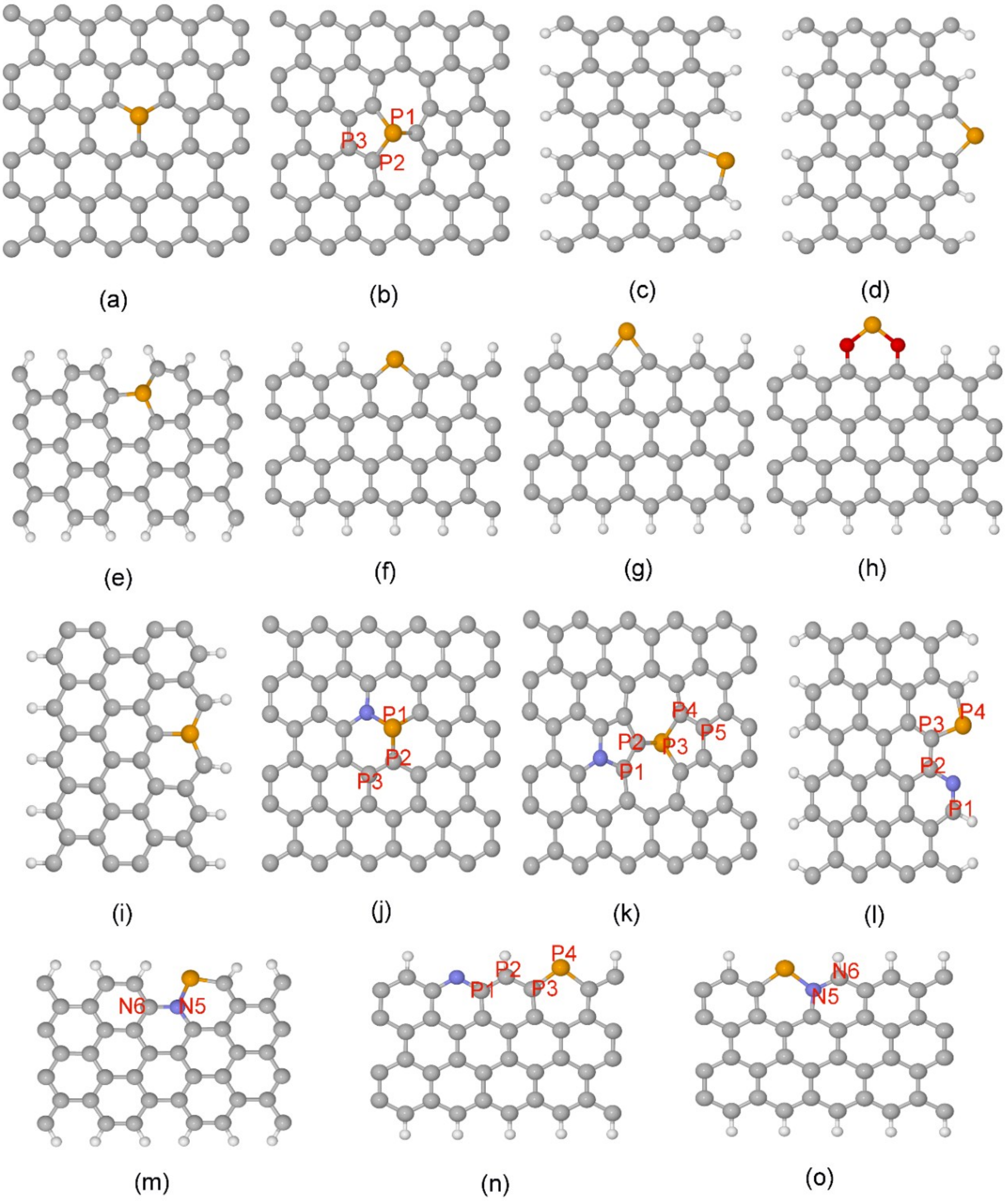

(a) (b) (c) (d)

(e) (f) (g) (h)

(i) (j) (k) (l)

(m) (n) (o)

Fig. S1. The structures of (a) G-P-1; (b) SW-P-1, SW-P-2, and SW-P-3; (c) A-P-1; (d) A-P-2; (e) A-P-3; (f) Z-P-1; (g) Z-P-2; (h) Z-P-3; (i) Z-P-4; (j) G-PN-1, G-PN-2, and G-PN-3; (k) SW-PN-1, SW-PN-2, SW-PN-3, SW-PN-4, and SW-PN-5; (l) A-PN-1, A-PN-2, A-PN-3, and A-PN-4; (m) A-PN-5 and A-PN-6; (n) Z-PN-1, Z-PN-2, Z-PN-3, and Z-PN-4; (o) Z-PN-5 and Z-PN-6. The white, grey, blue, red, and brown spheres denotes for H, C, N, O, and P atoms.

2. Limiting potential calculations

The limiting potentials for ORR and OER are defined as follows:

$$U_{\mathrm{ORR}} = Mini[-\Delta G_{\mathrm{i}}]/ne \qquad (S2)$$

$$U_{\mathrm{OER}} = Max[\Delta G_{\mathrm{i}}]/ne \qquad (S3)$$

where n is the number of electrons transferred for each electrochemical step and e is the elementary charge. The meaning of the *Mini* and *Max* of the above equation are to select the smallest and largest value in the brackets. ΔG_{i} is the free energy variation of each elementary step.

The free energy variation can be obtained by DFT total energy calculations by adding corrections for zero point energy, entropy and solvation energy. The total energies of intermediates are calculated and converted to free energies by adding some corrections:

$$\Delta G = \Delta E_{\mathrm{Total}} + \Delta E_{\mathrm{ZEP}} - T\Delta S + \Delta G_{\mathrm{s}} \qquad (S4)$$

where E_{Total} is the calculated total energy by DFT, ΔE_{ZPE} is zero point energy, ΔS is entropy that employed as the previous paper[1], and ΔG_{s} is solvation energy. The solvation energy is -0.22 eV for *OH and *OOH intermediates of ORR as the O in H_2O molecule would toward the electrode due to the direction of electric field for ORR, and it is -0.22 eV for *O, *OH and *OOH intermediates of OER as H in H_2O molecule would toward the electrode due to the difference of electric field direction for OER process.

3. Experimental details

3.1 Chemicals. The following chemicals were used as received without modification: graphite (<20 micron, Sigma-Aldrich), sulfuric acid (95-97%, Merck KGaA), potassium permanganate (99+%, Sigma-Aldrich), hydrogen peroxide aqueous solution (30wt%, Sigma-Aldrich), diammonium phosphate (DAP, Sigma-Aldrich), ammonium dihydrogen phosphate (ADP, Sigma-Aldrich), aqueous cyanamide solution (50 wt%, Sigma-Aldrich), Nafion (5 wt.% in alcohol and water, Sigma-Aldrich), 20% platinum on carbon black (Alfa Aesar), and 20%

iridium on Vulcan (Fuel Cell Store).

3.2 Preparation of a graphene oxide. Graphite oxide (GO) was synthesized by a modified Hummer method, as previously reported.[2] The graphene oxide aqueous solution (2 mg ml^{-1}) was achieved by continuous probe sonication (Hielscher UP400) of a mixture of 1 g GO and 500 mL DI H_2O for 24 hours, followed by centrifugation (Heraeus Biofuge Primo) at 8000 RPM for 30 min to remove any trace amount of unexfoliated GO.

3.3 Preparation of P,N co-doped graphene framework. The phosphorus and nitrogen co-doped graphene frameworks (PNGF) are prepared via a one-pot hydrothermal reaction using graphene oxide as the carbon source, diammonium phosphate (DAP) or ammonium dihydrogen phosphate (ADP) as the single phosphorus and nitrogen precursors, and cyanamide (CA) as an extra nitrogen precursor, followed by the freeze-drying and with / without the high-temperature calcination. The achieved samples are named as PNGF_DAP, PNGF_ADP, PNGF_ADP(op), PNGF(op), respectively, according to their corresponding synthesis conditions. More specifically, in order to form PNGF_DAP or PNGF_ADP, 396 mg DAP (3 mmol) or 345 mg ADP (3 mmol) was added into 15 ml graphene oxide (2 mg ml^{-2}), and the mixture was sonicated for 30 min before being moved into a Teflon-lined stainless steel autoclave for hydrothermal reaction at 180 °C for 12 h. The formed hydrogel was freeze-dried for 24 h. The thermal annealing to achieve PNGF_DAP_800 conduced at 800 °C for 1 h under flowing nitrogen (ramping rate was 3 $°C.min^{-1}$). The PNGF_ADP(op) was synthesized via a similar route as PNGF_ADP but using a smaller amount of ADP (132 mg, 1 mmol). The PNGF(op) was synthesized via a similar route as PNGF_ADP(op) but adding CA (240 μl) as an extra nitrogen precursor in the hydrothermal reaction.

3.4 Physical and Electrochemical Characterizations. The nitrogen and phosphorus binding configurations were analyzed by X-ray photon spectroscopy (Thermo Scientific K-Alpha). Rotating Disk Electrode (RDE) measurements were conducted in O_2-saturated 0.1M KOH. Oxygen was purged for at least 30 minutes before the measurement and was continuously bubbled through the electrolyte during the tests, in order to ensure the saturation of the electrolyte with O_2. RDE (glass carbon tip, Metrohm) was used as the working electrode, Ag/AgCl (sat. KCl, Metrohm) as the reference electrode and a platinum sheet (Metrohm) as the counter electrode. The scan rate for rotating voltammetry was 10 mV s^{-1}. All the results were recorded using Metrohm Autolab 302N and Metrohm Multi Autolab. The potentials reported in this work were converted with reference to the reversible hydrogen electrode (RHE) scale by the addition of a value of 0.965 V.

For preparation of the RDE working electrode, 4 mg catalyst and 40 µl Nafion solution (5 wt%) were added in 3 ml de-ionized water, followed by sonication for 60 minutes to achieve uniform dispersion of the catalysts in the solvent. Catalyst suspension (5.4 µl) was drop-casted on the RDE tip (3 mm diameter) and dried at 60 °C. The catalyst loading is ca. 0.1 mg cm^{-2} for all samples, including the commercial Pt/C and Ir/C.

The electron transfer number (ETN, n) was calculated based on the Koutecky–Levich (K-L) equation:

$$\frac{1}{J}=\frac{1}{J_L}+\frac{1}{J_K}=\frac{1}{0.2nFC_0D_0^{2/3}v^{-1/6}\omega^{1/2}}+\frac{1}{J_K} \qquad (S5)$$

where J is the measured current density, J_{L} and J_{K} are the diffusion limiting and kinetic current density, F is the Faraday constant (96485 sA.mol^{-1}), C_0 is the bulk concentration of dissolved O_2 in 0.1M KOH (1.2×10^{-3} mol.L^{-1}), D_0 is the diffusion coefficient of O_2 in 0.1M KOH (1.9×10^{-5} $cm^2.s^{-1}$), v is the kinematic viscosity of the electrolyte (0.01 $m^2.s^{-1}$), and ω is the angular velocity (in RPM).

Therefore, the diffusion corrected kinetic current density (J_K) was calculated on the basis of the K-L equation as well:

$$J_K=\frac{J.J_L}{J_L-J} \qquad (S7)$$

The potential cycling was conducted between 0.2 and 1.2 V vs. RHE for ORR or between 1.2 and 2 V vs. RHE for OER, using a scan rate of 100 mV.s^{-1} for 5000 cycles. The Chronoamperometry measurement was conducted at the potentials under which the current density reached 3 or 10 mA cm^{-2} at 1600 rpm for ORR and OER, respectively, and lasted for 20 hours in total.

4. LSV, K-L plots, Chronoamperometry and XPS

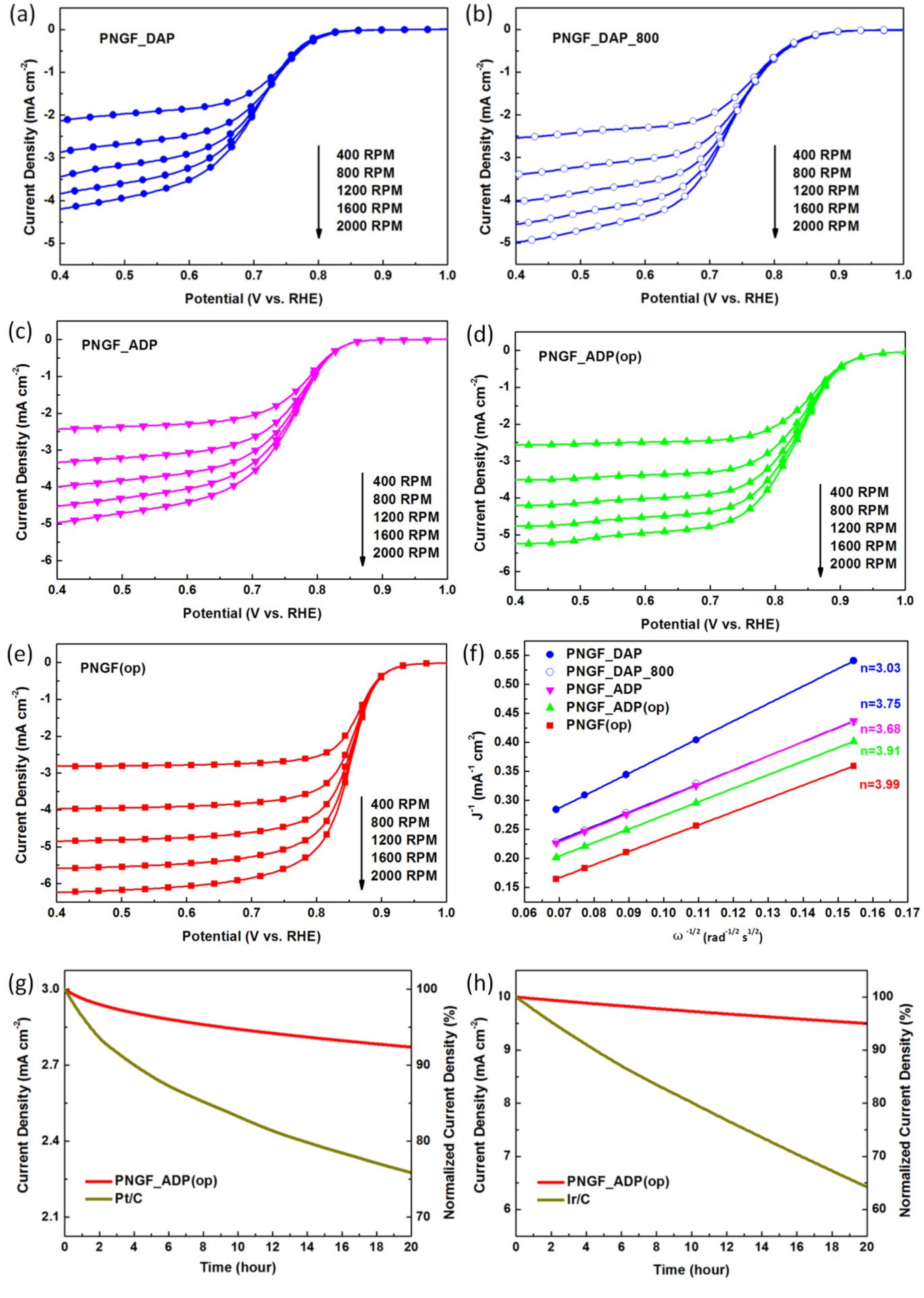

Fig. S2. ORR linear sweep voltammograms (LSV) for (a) PNGF_DAP, (b) PNGF_DAP_800, (c) PNGF_ADP, (d) PNGF_ADP(op), and (e) PNGF(op) from 400 to 2000 RPM. (f)

Koutecky-Levich plots of PNGF_DAP, PNGF_DAP_800, PNGF_ADP, PNGF_ADP(op) and PNGF(op) at 0.6 V vs. RHE, derived from the above LSV in Fig. S2 (a) to (e). Chronoamperometry measurement of (g) ORR stability for PNGF(op) and Pt/C and (h) OER stability for PNGF(op) and Ir/C.

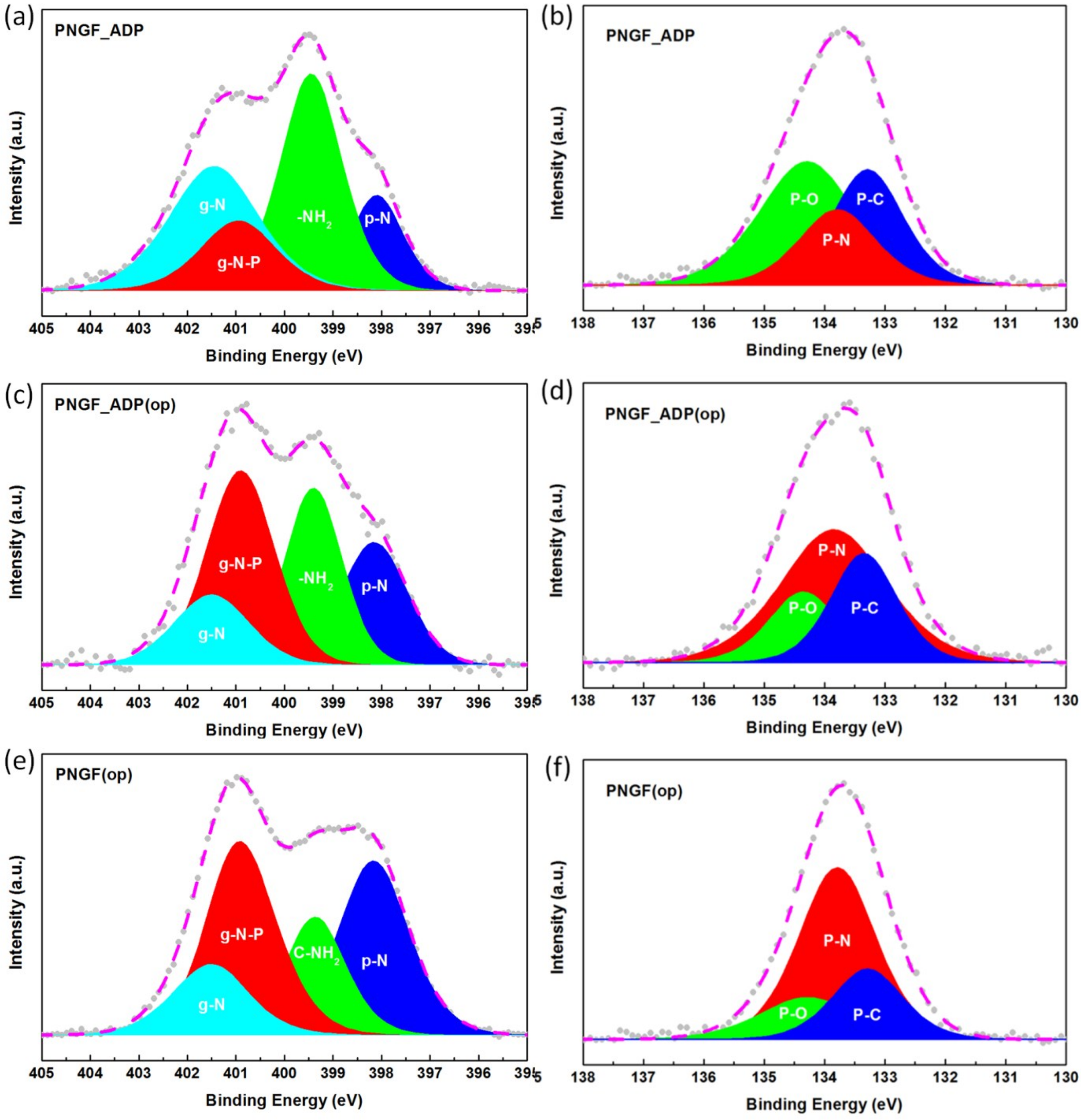

Fig. S3. XPS N1s and P2p spectra for (a-b) PNGF_ADP, (c-d) PNGF_ADP(op) and (e-f) PNGF(op).

5. Density of States (DOS) for different structures

The density of states (DOS) for different types of P/N doped carbon material structures were calculated and shown as followings. The DOS at valence band maximum (VBM) and the conduction band minimum (CBM) are related with activity for ORR/OER. The projected density of states (PDOS) of some important atoms are displayed separately. The sites with high DOS/PDOS around the VBM/CBM are selected as a possible active site for ORR/OER.

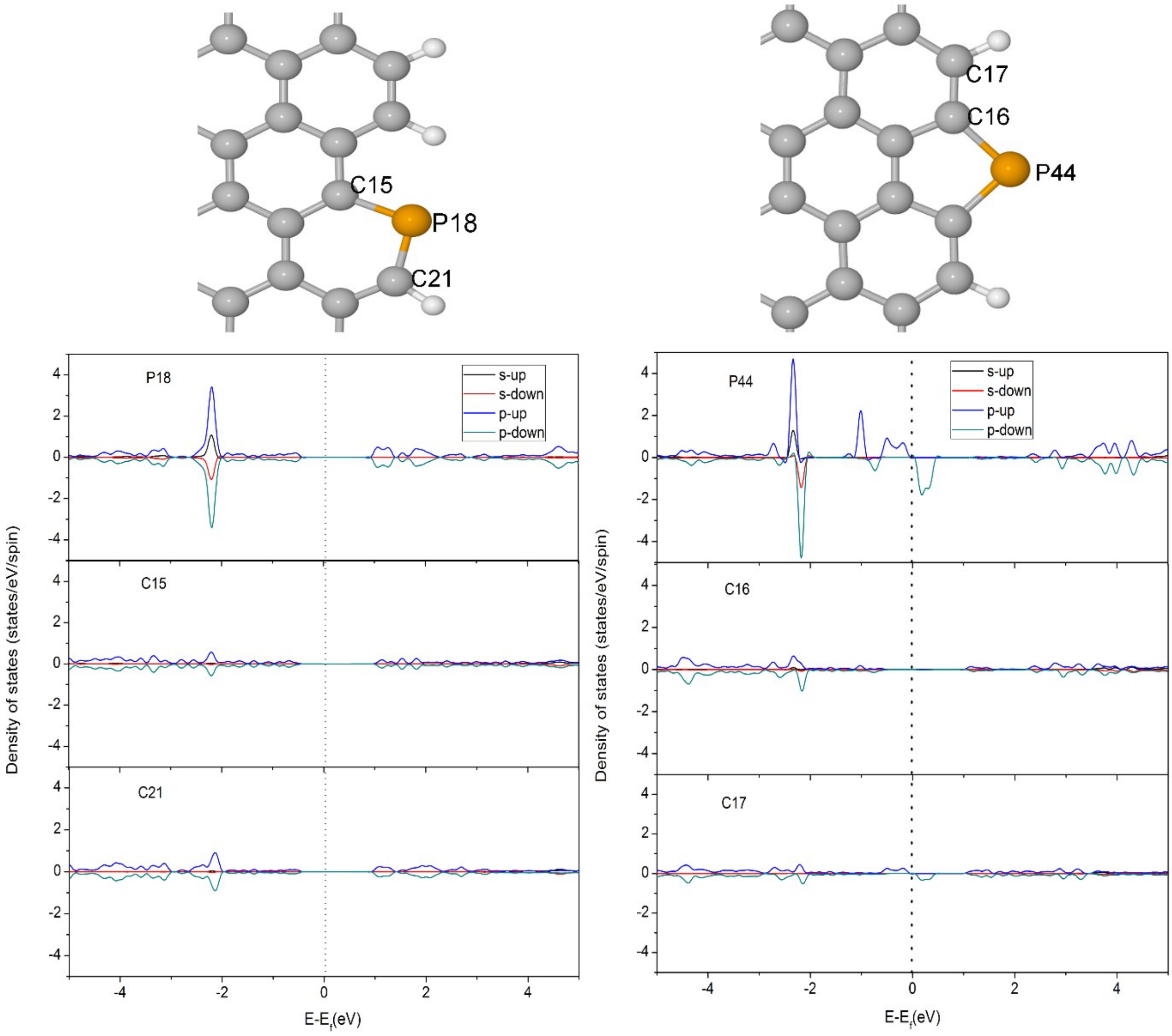

Fig. S4. The PDOS of A-P-1 and A-P-2. The P atom sites are selected as possible active sites.

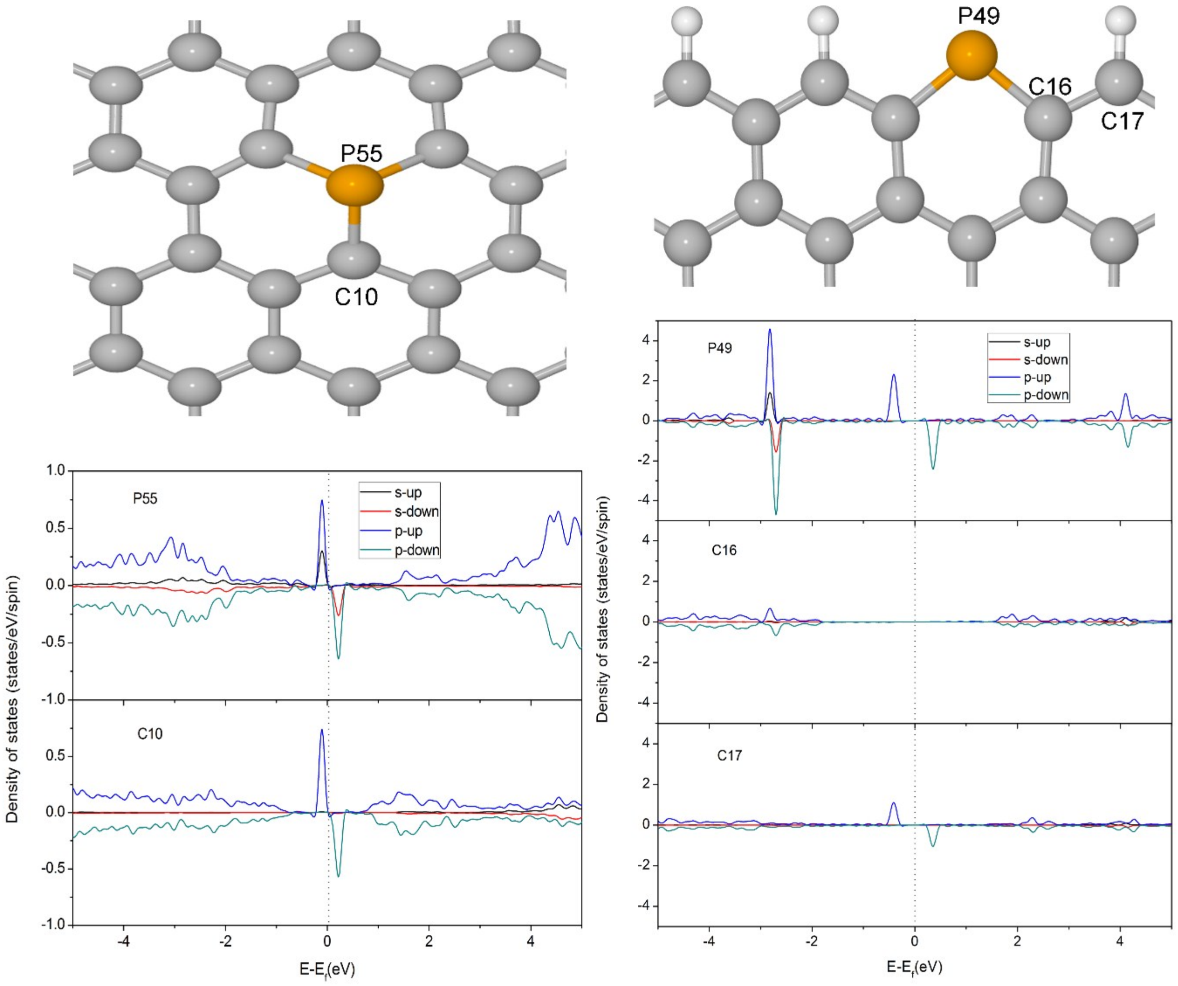

Fig. S5. The PDOS of G-P-1 and Z-P-1. The P atom sites are selected as possible active sites.

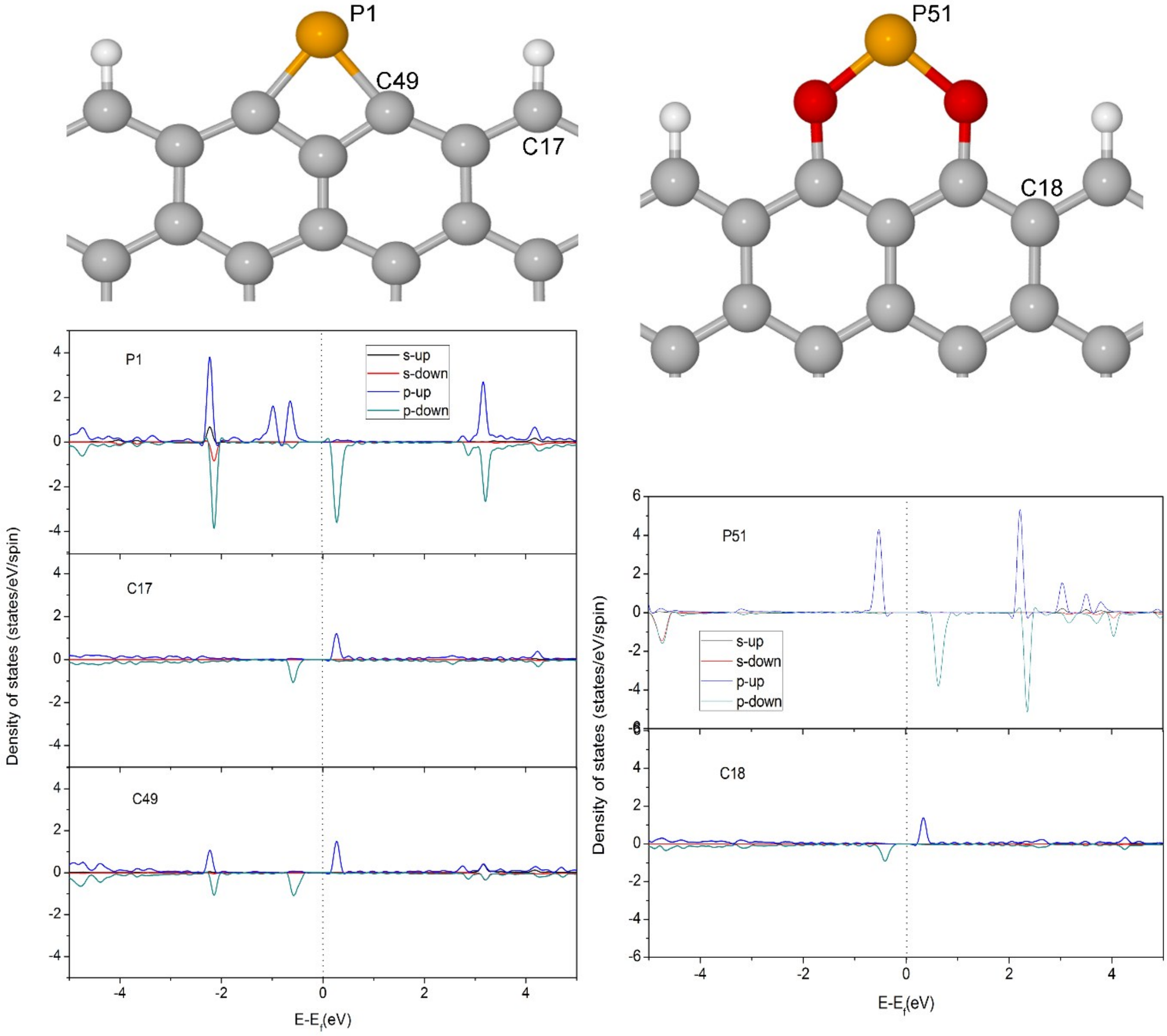

Fig. S6. The PDOS of Z-P-2 and Z-P-3. The P atom sites are selected as possible active sites.

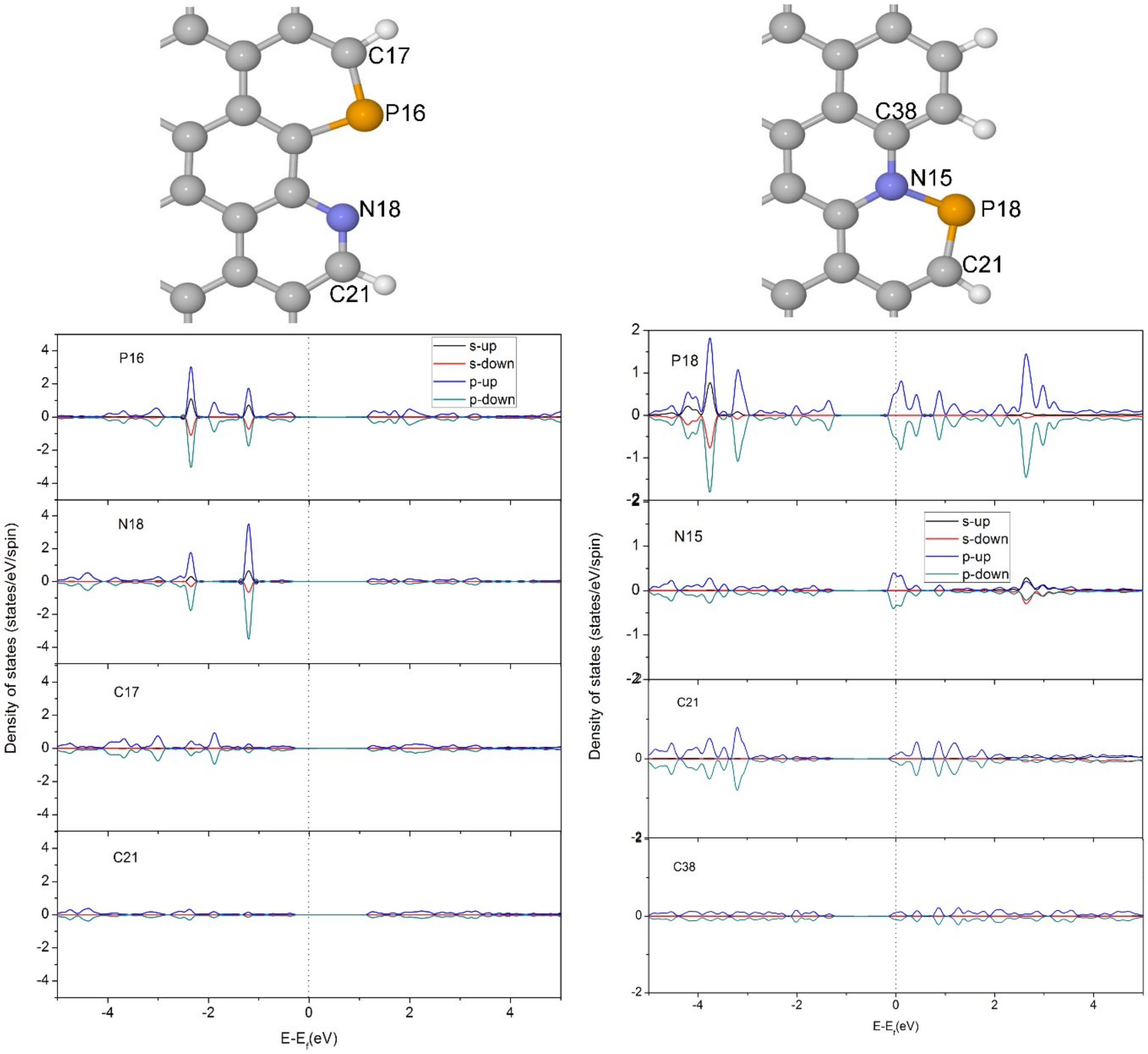

Fig. S7. The PDOS of A-PN-4 and A-PN-5. The P atom sites are selected as possible active sites.

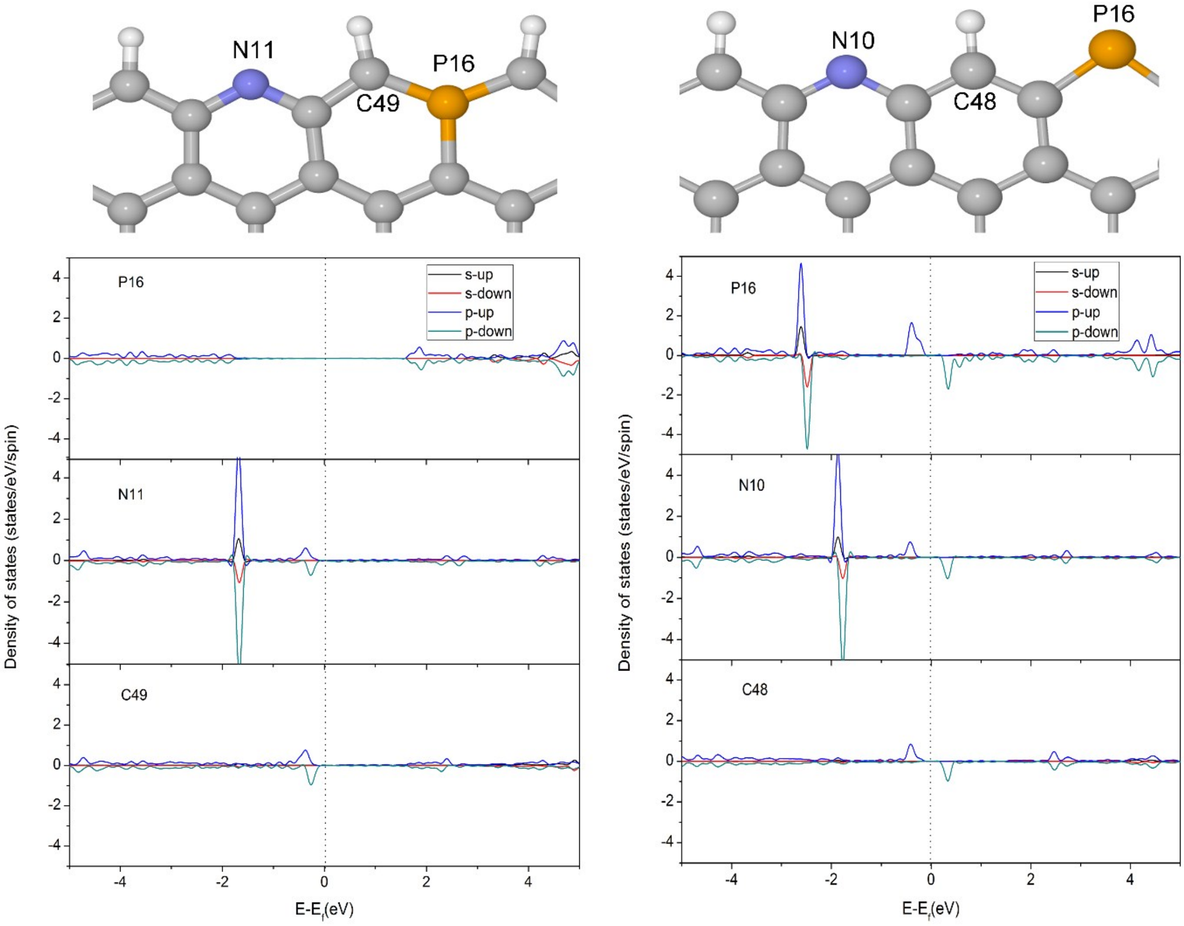

Fig. S8. The PDOS of Z-PN-3 and Z-PN-4. The C49 and P atom sites are selected as possible active sites.

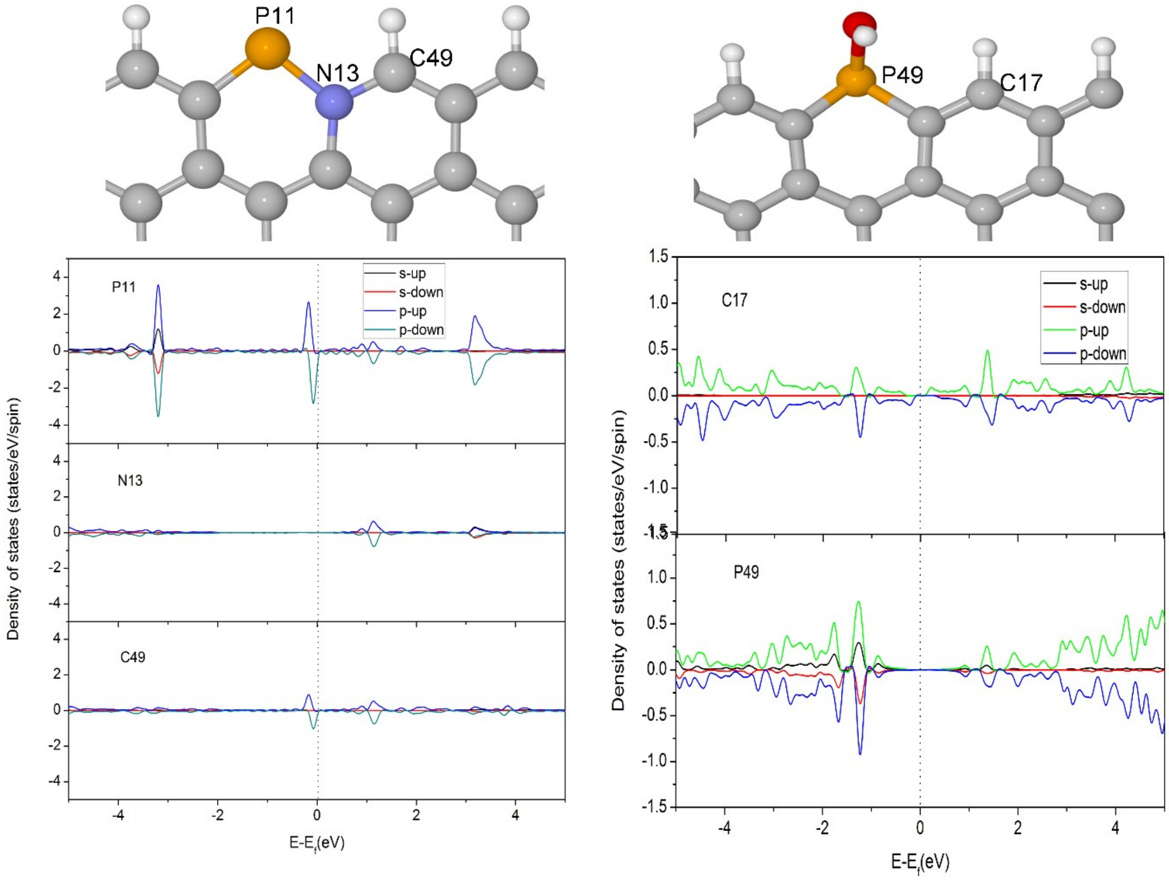

Fig. S9. The PDOS of Z-PN-5 and Z-P-1-OX1. The P atom sites are selected as possible active sites.

6. Curvature effect for ORR/OER

In order to tune the ORR/OER limiting potentials, curvature effect are checked for the Z-PN-5-OX2 and Z-PN-5-rm structures. The results are shown in **Fig. 3** in the main text. The curvatures are introduced in graphene structures by reducing the lattice parameters along the zigzag edge direction as shown in **Fig. S10**. Strain is produced after the lattice parameter is reduced, which would make the structure generate curve structure as shown below. The curvature is denoted by percentage of lattice parameter reduced, which is ranged from 0% and 23%. The curvature with parameters reduced below 20% should be realized by using carbon nanotubes or porous carbon structures, while too large curvature may difficult to realize.

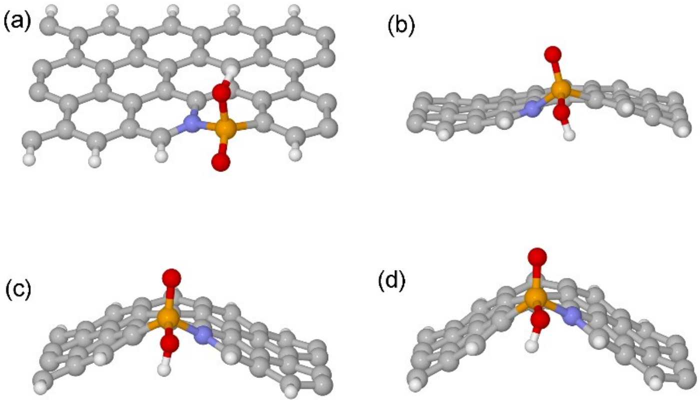

Fig. S10. Structures for Z-PN-5-OX2 with different curvature: (a) 0%, (b) 3.1%, (c) 7.1%, and (d) 11.1%. The white, grey, blue, red, and brown spheres denotes for H, C, N, O, and P atoms.

7. XPS Binding Energy Simulation

The theoretical X-ray photoelectron spectroscopy (XPS) was simulated according to the total energy difference (ΔSCF) method by using CP2K code as mentioned in the main text. Different types of active sites are shown in Fig. S11. The simulated P2p XPS binding energy of Z-PN-5-OX2 structure is 133.5 eV, which agrees well with the experimentally measured binding energy of P-N structures (ca. 133.7 eV, Fig. 3 (e)). The simulated N1s XPS binding energy of the g-N-P peak is also 0.5 eV more negative than that of g-N, in accordance with the experimental values as well. Other the XPS peak positions of other active sites such as -NH_2 and p-N have been well studied in previous experimental measurement and thus the corresponding simulations are not presented here.

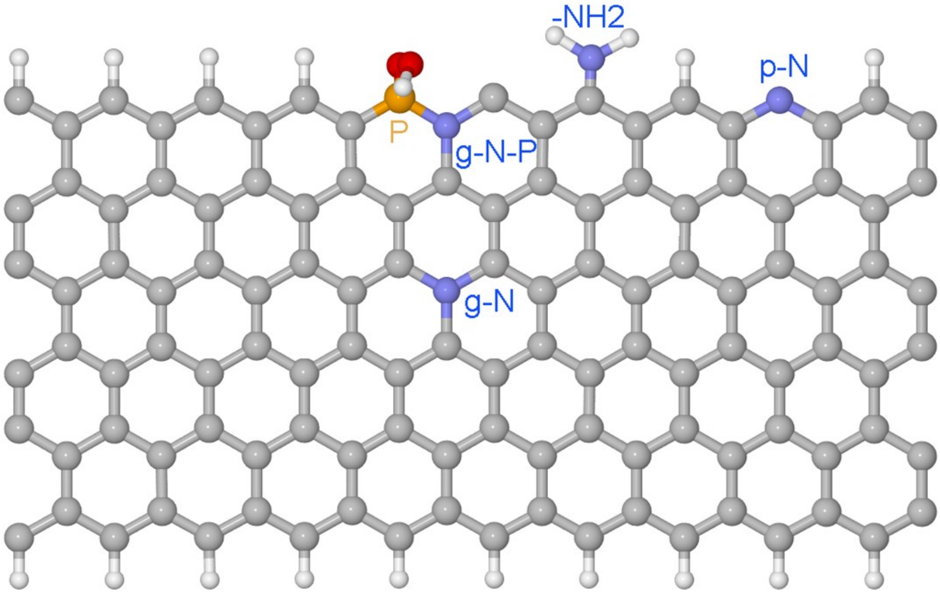

Fig. S11. The supercell and local atomic structures for different types of active sites. Note here that only one type of sites is included in the supercell for each specific simulation.

References

1 G. L. Chai, Z. F. Hou, D. J. Shu, T. Ikeda and K. Terakura, *J. Am. Chem. Soc.,* 2014, **136,** 13629-13640.

2 K. Qiu, G. Chai, C. Jiang, M. Ling, J. Tang, Z. Guo. *ACS Catal.,* 2016*,* **6,** 3558-3568.